


2023

TELP Theory: Elucidating the Major Observations of Rieger et al. 2021 in Mitochondria

James Weifu Lee
Old Dominion University, jwlee@odu.edu

Follow this and additional works at: https://digitalcommons.odu.edu/chemistry_fac_pubs

 Part of the [Cell Anatomy Commons](#), [Molecular, Cellular, and Tissue Engineering Commons](#), [Organic Chemistry Commons](#), and the [Physical Chemistry Commons](#)

Original Publication Citation

Lee, J. W. (2023). TELP theory: Elucidating the major observations of Rieger et al. 2021 in mitochondria. *Mitochondrial Communications*, 1, 62-72. <https://doi.org/10.1016/j.mitoco.2023.09.001>

This Article is brought to you for free and open access by the Chemistry & Biochemistry at ODU Digital Commons. It has been accepted for inclusion in Chemistry & Biochemistry Faculty Publications by an authorized administrator of ODU Digital Commons. For more information, please contact digitalcommons@odu.edu.



TELP theory: Elucidating the major observations of Rieger et al. 2021 in mitochondria

James Weifu Lee

Department of Chemistry and Biochemistry, Old Dominion University, Norfolk, VA, 23529, USA

ARTICLE INFO

Keywords:

Protonic capacitor
Water as protonic conductor
Proton “hops and turns” mechanism
Excess protons
Transmembrane-electrostatically localized protons (TELP)
Local protonic motive force
ATP synthesis

ABSTRACT

The transmembrane-electrostatically localized protons (TELP) theory may represent a complementary development to Mitchell's chemiosmotic theory. The combination of the two together can now excellently explain the energetics in mitochondria. My calculated transmembrane-attractive force between an excess proton and an excess hydroxide explains how TELP may stay within a 1-nm thin layer at the liquid-membrane interface. Consequently, any pH sensor (sEcGFP) located at least 2–3 nm away from the membrane surface will not be able to see TELP. This feature as predicted from the TELP model was observed exactly in the experiment of Rieger et al., 2021. In contrast to their belief “the Δp at ATP synthase is almost negligible under OXPHOS conditions”, I find, when TELP activity is included in the energy calculations, there is plenty of total protonic Gibbs free energy (ΔG_T) well above the physiologically required value of $-24.5 \text{ kJ mol}^{-1}$ to drive ATP synthesis through F_0F_1 -ATP synthase.

1. Introduction

In the journal *EMBO reports* (2021), Rieger et al. reported a wonderful pH-sensing GFP mitochondrial experiment,¹ where “pH profiles of mitochondrial sub-compartments were recorded with high spatial resolution in live mammalian cells by positioning a pH sensor directly at ATP synthase's F_1 and F_0 subunits, complex IV and in the matrix”. The Rieger et al., 2021 publication states: “for on-side pH determination, the pH-sensitive GFP derivative sEcGFP,² also known as pHluorin, was used as a ratiometric pH sensor.³⁴ The generated pH profiles revealed that the local Δp was unexpectedly low under OXPHOS (oxidative phosphorylation), which are ATP synthesis conditions”.¹ Remarkably, the intracristal liquid pH 7.3 and the extracristal liquid pH 7.4 as measured by Rieger et al., 2021 with SU γ -sEcGFP and SU e-sEcGFP were in excellent agreement with the intracristal bulk-liquid phase pH_{pB} of “7.25” and the extracristal bulk-liquid phase pH_{nB} of “7.35” that were employed in my previously published mitochondrial energetics studies.^{5–7}

The Rieger et al., 2021 experimental pH profiling observations of mitochondrial sub-compartments¹ can now be better explained with the concept of a “protonic capacitor” across the mitochondrial crista membrane according to the fundamentals of the transmembrane-electrostatically localized proton (TELP) theory.^{5,8} The TELP theory was developed with the application of Gauss law^{9–11} based

on the understanding of liquid water as a protonic conductor: protonic conduction through the “hops and turns” mechanism (Fig. 1) as first outlined by Grotthuss.^{12–15}

Recently, TELP activity has been experimentally demonstrated using a biomimetic water-membrane-water system^{16–19} showing how a “protonic capacitor” can form from excess protons at one side of a membrane with excess hydroxides at the other side of the membrane. To account for the TELP activity, Lee has recently formulated a new series of protonic motive force (pmf) equations⁶ as follows.

$$\text{pmf} = \Delta\psi + \frac{2.3 RT}{F} \log_{10} \left(\frac{[H_{pB}^+]}{[H_{nB}^+]} \right) + \frac{2.3 RT}{F} \log_{10} \left(1 + \frac{[H_L^+]}{[H_{pB}^+]} \right) \quad (1)$$

Here $\Delta\psi$ is the transmembrane potential from the positive (p)-side to the negative (n)-side as defined by Mitchell,^{20,21} Nicholls and Ferguson^{22,23}; R is the gas constant; T is the temperature in Kelvin; F is the Faraday constant; $[H_L^+]$ is the TELP concentration at the liquid-membrane interface on the p -side of the membrane; $[H_{pB}^+]$ is the “proton concentration in the bulk aqueous p -phase” (intermembrane space and cristae space in the case of mitochondria); and $[H_{nB}^+]$ is the “proton concentration in the bulk liquid n -phase” (matrix in mitochondria).⁵

As discussed previously,⁶ the first two terms of Eq. (1) comprise the

E-mail address: jwlee@odu.edu.

<https://doi.org/10.1016/j.mitoco.2023.09.001>

Received 27 July 2023; Received in revised form 19 September 2023; Accepted 28 September 2023

Available online 5 October 2023

2590-2792/© 2023 The Authors. Publishing services by Elsevier B.V. on behalf of KeAi Communications Co. Ltd. This is an open access article under the CC BY license (<http://creativecommons.org/licenses/by/4.0/>).

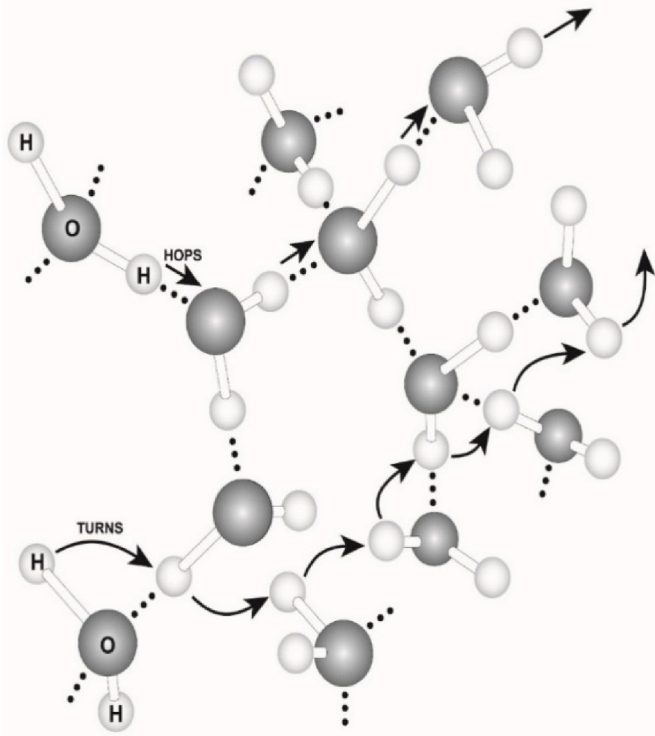


Fig. 1. Liquid water as a protonic conductor: Protons can quickly translocate among water molecules by the “hops and turns” mechanism which is also known as the Grotthuss mechanism.¹⁵ (Adapted from Lee 2012 *Bioenergetics* 1: 104, 1–8).

“Mitchellian bulk phase-to-bulk phase proton electrochemical potential gradients” now called as the “classic” pmf; whereas the last term is the “local” pmf from TELP as presented more clearly in the following local pmf equation.

$$\text{local pmf} = \frac{2.3 RT}{F} \log_{10} \left(1 + \frac{[H_L^+]}{[H_{pB}^+]} \right) \quad (2)$$

As shown in Eq. (2), the local pmf is related to the ratio ($[H_L^+]/[H_{pB}^+]$) of TELP concentration $[H_L^+]$ at the liquid-membrane interface to the bulk liquid-phase proton concentration $[H_{pB}^+]$ at the same p -side of the membrane.

According to the protonic capacitor concept,⁸ the ideal TELP concentration $[H_L^+]^0$ on the p -side of the membrane is a function of the transmembrane potential $\Delta\psi$ as expressed in the following equation:

$$[H_L^+]^0 = \frac{C}{S} \cdot \frac{\Delta\psi}{l \cdot F} \quad (3)$$

where C/S is “the specific membrane capacitance per unit surface area”, l is “the thickness of TELP layer”,²⁴ and F is the Faraday constant.

The TELP concentration $[H_L^+]$ at the equilibrium state of cation-proton exchange with each of the cation species M_{pB}^{i+} of the bulk liquid p -phase is,

$$[H_L^+] = \frac{[H_L^+]^0}{\prod_{i=1}^n \left\{ K_{p_i} \left(\frac{[M_{pB}^{i+}]}{[H_{pB}^+]} \right) + 1 \right\}} \quad (4)$$

Here $[M_{pB}^{i+}]$ is the non-proton cation (such as Na^+) concentration in the bulk liquid p -phase, and K_{p_i} is the equilibrium constant for the cation to exchange with TELP.

The TELP model with Eqs. (1)–(4) is useful in elucidating real-world

bioenergetic systems with both delocalized and localized protonic coupling. For example, it has been successfully applied in elucidating the decades-longstanding energetic conundrum^{25–27} of ATP synthesis in alkaliphilic bacteria^{28–33} and in bettering the understanding of energetics in mitochondria.^{6,8} Its application has recently led to the identification of the TELP thermotrophic function as the Type-B energetic process^{34–37} which can isothermally utilize environmental heat energy to do useful work in helping drive the synthesis of ATP.^{6,7}

The application of the TELP model has also successfully elucidated the energetic significance of mitochondrial cristae formation. It has calculated, for the first time, the numbers of transmembrane-electrostatically localized protons to be in a range from 1.84×10^4 to 7.36×10^4 protons per mitochondrion, corresponding to a range of transmembrane potential $\Delta\psi$ from 50 to 200 mV for a mitochondrion.⁸ The application of the TELP model has now also resulted in a novel neural membrane potential equation²⁴ based on the transmembrane-electrostatically localized protons/cations (TELC) capacitor concept with deep insights for neuronal electrophysiology, that may represent a complementary development to the classic Goldman-Hodgkin-Katz equation.

Certain scholars including a special Collection editor for the Nature research journal *Scientific Reports* are now able to understand and appreciate the TELP research progresses. In her latest editorial,³⁸ the editor has acknowledged that the TELP research progresses “refined and improved our knowledge of transport bioenergetics” in addition to the discovery of the TELP thermotrophic function.

With the TELP theory, we successfully elucidated the effect of transient “excess protons” in the experiment of Pohl’s lab group.³⁹ Previously, the results of Pohl’s lab group experiment³⁹ were somehow used (or misunderstood) as a “support” to the putative “potential barrier model” of Junge and Mulikidjanian.^{40,41} For example, Silverstein⁴² once claimed that the putative “potential barrier model” of Junge and Mulikidjanian^{40,41} was “supported by Pohl’s group”³⁹. In his previous article,⁴³ Silverstein even claimed it “seems to rule out Lee’s model”. In contrast, as shown in my recent publication,⁴⁴ the experimental results of Pohl’s group³⁹ can actually be well explained by the protonic conduction fundamentals with the TELP model,^{5,8} but cannot really be explained by the putative “potential barrier model” of Junge and Mulikidjanian.^{40,41} Remarkably, this new finding with the TELP theory agrees well with the independent analysis on the Pohl’s lab group experimental results³⁹ by Agmon and Gutman,⁴⁵ which also concluded “the excess protons propagate as an advancing front”.

In this article, we will elucidate the Rieger et al., 2021 experimental pH profiling observations of mitochondrial sub-compartments.¹ Especially, we will employ TELP property to explain why a sEcGFP pH sensor at least 2–3 nm away from membrane surface can detect bulk liquid-phase pH but cannot see TELP. The TELP-associated protonic capacitor formation in a mitochondrial crista will be mathematically justified by application of the Gauss Law equation. Using the transmembrane attractive force between an excess proton and an excess hydroxide, which was calculated to be as much as 1.92×10^{-11} newton (N),²⁴ we will provide a physical explanation how TELP activity stays within a 1-nm thin layer on membrane surface so that the sEcGFP pH sensors at least 2–3 nm away from membrane surface can see bulk liquid pH but not TELP. Rieger et al., 2021 made some interesting conclusion “Strikingly, the Δp at ATP synthase is almost negligible under OXPHOS conditions” with their experimental observation but apparently without fully considering the TELP theory.^{5,6,8} When the contribution from TELP activity is included in the energy calculation (Eqs. (1)–(7)) near the end of this article, readers will also be able to see that there is plenty of total protonic Gibbs free energy (ΔG_T) well above the physiologically required value of $-24.5 \text{ kJ mol}^{-1}$ to drive ATP synthesis through the F_0F_1 -ATP synthase in mitochondria. Consequently, the experimental observations of Rieger et al., 2021 under the OXPHOS conditions will now be better elucidated with the fundamentals of the TELP model,^{5,8} which is fundamentally important to the science of energetics.

2. Results and discussion

2.1. TELP model for a mitochondrial crista driving protonic energetic process for ATP synthesis

According to our study here, the mitochondrial crista bioenergetic functions can now be explained with the fundamentals of the TELP model^{5,8} as illustrated in Fig. 2. As the redox-driven respiratory complexes I, III and IV pump protons across the membrane from the mitochondrial matrix side to the intracristal side, it will create a population of excess protons at the intracristal side while leaving excess hydroxides at matrix side. The excess hydroxides will stay at the liquid-membrane interface along the matrix side while transmembrane-electrostatically attracting the excess protons of the other side to the intracristal membrane surface, which thus forms an “excess hydroxides-membrane-excess protons” capacitor (Fig. 2).

As shown in Fig. 2, the TELP at the liquid-membrane interface around crista membrane surface is well positioned to drive ATP synthase to produce ATP from ADP and Pi. Notably, the protonic inlet of ATP synthase is perfectly located within the TELP layer on crista membrane surface for effective utilization of TELP in driving the synthesis of ATP as shown previously.^{6,33} This explains how the energetic system functions together with TELP to drive ATP synthesis.

As reported previously,^{5,6,8,46} this TELP model (Fig. 2) is based on the knowledge of liquid water as a protonic conductor: protonic conduction through the “hops and turns” mechanism (Fig. 1) as outlined first by Grothuss.^{12–15} That is, in regarding protonic conduction, the liquid water on the matrix side is a protonic conductor; the membrane is an insulator; and the liquid water in the intracristal space is also a protonic conductor. Consequently, this protonic conductor-insulator-conductor system is a protonic capacitor by the physical definition.

This protonic capacitor can be mathematically justified by using the

Gauss Law equation of electrostatics and the fact that there can be no electric field E inside a protonic conductor (Fig. 2). Gauss’s Law relates the net charge Q within a volume to the flux of electric field lines through the closed surface surrounding the volume in the following equation, as shown in Ref. 46,47,

$$\epsilon_0 \oint \mathbf{E} \cdot d\mathbf{S} = Q \tag{5}$$

where ϵ_0 is the value of the absolute dielectric permittivity of classical vacuum and $d\mathbf{S}$ is a differential surface element. Here the small circle on the integral sign indicates that the integration is performed over the closed surface. Consider then a series of integration applications, where a small volume at the center of the intracristal liquid is gradually increased until it is just inside the intracristal liquid space in Fig. 2. The electric field E is zero within a proton-conductive liquid body. Thus, in each case the left side of Eq. (5) vanishes and therefore the right side must also vanish, which means that no net charge ($Q = 0$) is within the volume; the excess protons in this case must therefore be at the intracristal water-membrane interface along the p -side of the inner mitochondrial membrane.

Conversely, the electric field $E = 0$ holds true everywhere also within the extracristal (matrix) liquid environment. Applying Gauss’s Law to a series of volumes enclosing the entire crista system and decreasing them to be just outside the extracristal inner membrane surface (Fig. 2), the surface integrals of Eq. (5) vanish, and thus no net excess charge is found. Since the excess protons are at the intracristal side, the negative charges (excess hydroxides) must be at the extracristal membrane-water interface along the n -side of the crista membrane, precisely balancing the excess protons of the intracristal side, resulting in the total net charge of the entire system zero.

Note, in addition to the application of the Gauss Law equation as shown above that justifies the formation of an “excess hydroxides-

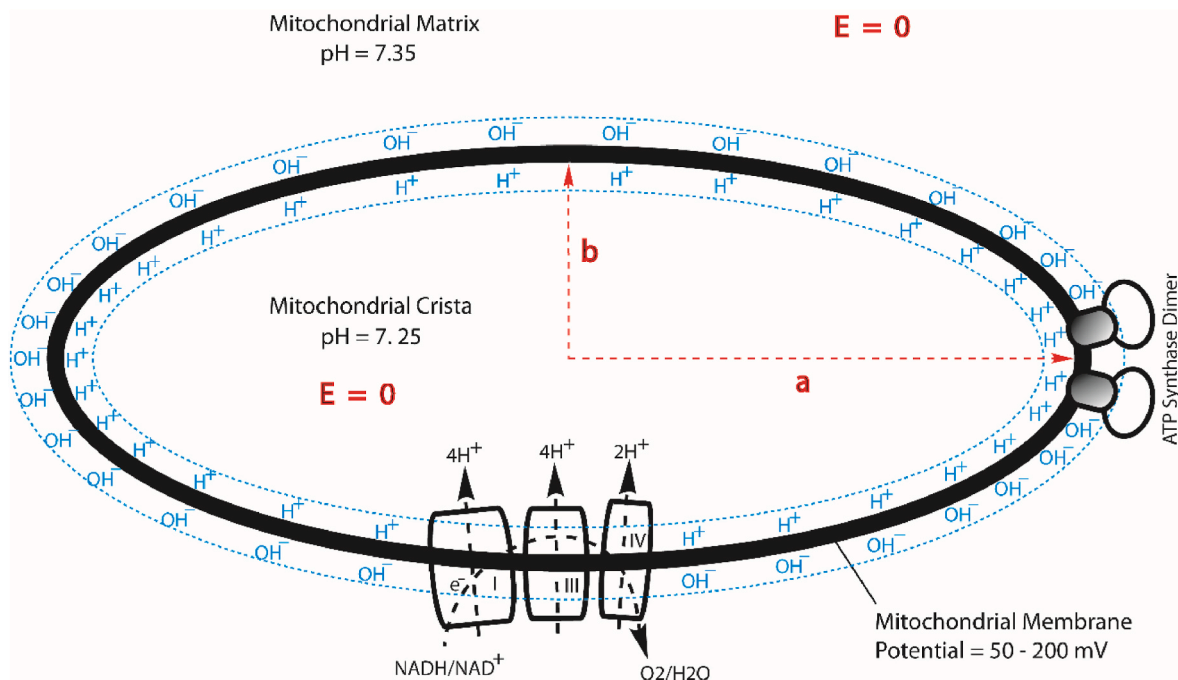


Fig. 2. The protonic membrane capacitor formation in a mitochondrial crista to drive ATP synthesis. The lateral asymmetric feature is resulted from the ellipsoidal geometric effect of a crista that enhances the density of TELP at a cristal tip where the F_0F_1 -ATP synthase enzymes are located in comparison with that of the relatively flat membrane region where the proton pumping complexes I, III and IV are located as illustrated in a cross section for an ellipsoidal-shaped mitochondrial crista. This cross section may be considered as a special result from the tri-axial (a, b, and c) protonic conducting ellipsoidal crista equation in 3-dimensional x, y, and z coordinates for its middle cross section (where the z coordinate is zero). This TELP (protonic capacitor) model also illustrates how excess protons (H^+) and hydroxides (OH^-) can be transmembrane-electrostatically localized along the two sides of mitochondrial inner membrane before proton-cation exchange as it could be in a water-membrane-water system. Adapted from Ref. 8.

membrane-excess protons” capacitor (Fig. 2) under the oxidative phosphorylation conditions in mitochondria, the protonic capacitor-based TELP equation (Eq. 3) shows the inter-relationship between the TELP concentration $[H_e^{+}]^0$ and the transmembrane potential (voltage) difference $\Delta\psi$. Technically, it is the TELP-associated membrane capacitor that gives rise to the transmembrane potential difference $\Delta\psi$. Consequently, if there is a substantial transmembrane potential difference $\Delta\psi$, there must be TELP. This fundamental understanding of the TELP theory may apply to many biological cells and membrane systems including mitochondria.

Furthermore, in addition to the TELP theoretical understanding 5,6,8,10,24,28,33,44 46, we recently have experimentally demonstrated the formation of an “excess hydroxides-membrane-excess protons” capacitor and its associated TELP activity using biomimetic “water-membrane-water” systems.^{16–18,48}

2.2. TELP model explaining why an sEcGFP pH sensor at least 2–3 nm away from membrane surface can detect bulk liquid pH but cannot see TELP

Rieger et al., 2021 performed a wonderful pH-sensing GFP experiment of mitochondrial sub-compartments (cristae) where “pH profiles of mitochondrial sub-compartments were recorded with high spatial resolution in live mammalian cells by positioning a pH sensor directly at ATP synthase’s F₁ and F₀ subunits, complex IV and in the matrix”.¹ In the experiment, Rieger et al., 2021 employed the pH-sensitive GFP derivative sEcGFP,² also known as pHluorin, which is a ratiometric pH sensor.³⁴ As shown in Fig. 3A, the pH sensor (sEcGFP) was fused through molecular genetic engineering to subunit of different oxidative phosphorylation (OXPHOS) complexes and to a mitochondrial processing peptidase (MPP) in the matrix. That is, they elegantly attached a pH sensor (sEcGFP) discreetly to the following positions: subunit Cox8a of the respiratory complex IV (CIV: Cox8a (CoxVIIIa)-sEcGFP), subunit e of complex V (CV SU e-sEcGFP), subunit γ of complex V (CV SU γ -sEcGFP),

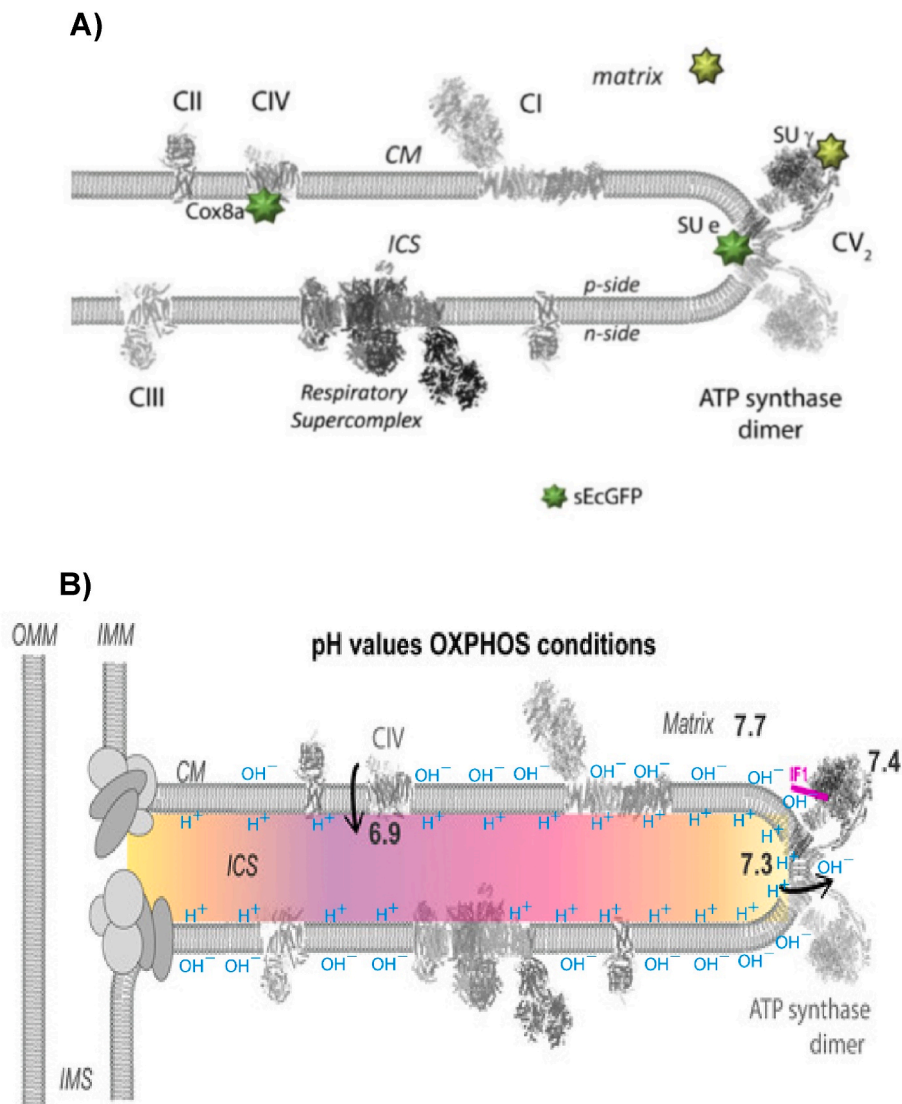


Fig. 3. A) Scheme showing the positions of the pH sensor (sEcGFP) fused to subunit of different oxidative phosphorylation (OXPHOS) complexes and the mitochondrial processing peptidase (MPP) in the matrix. CIV: Cox8a (CoxVIIIa)-sEcGFP; CV SU e-sEcGFP, CV SU γ -sEcGFP. Matrix: MPP-sEcGFP. CI: complex I, CII: complex II, CIII: complex III, CIV: complex IV, CV2: dimeric complex V. ICS: intracristal space, CM: crista membrane. B) Schematic drawing illustrates a protonic membrane capacitor with TELP along the intracristal membrane surface. The bulk-liquid pH values and resulting gradients under respiratory conditions were experimentally determined, where the color gradient was made following the ratiometric pH code employed throughout the study. Adapted and modified from Rieger et al. 2021.¹

and to the matrix protein mitochondrial processing peptidase (MPP-sEcGFP). The sEcGFP can be used as a ratiometric pH sensor since its pH-dependent emission spectra display an isobestic point (Gao et al., 2004; Rieger et al., 2014). Upon excitation with 405 nm, the emissions in two channels were simultaneously recorded, and their ratio was calculated ($\lambda_{511}/\lambda_{464}$) to determine pH value. The pH sensors MPP-sEcGFP, CoxVIIIa-sEcGFP, SU γ -sEcGFP, and SU e-sEcGFP positioned as indicated in Fig. 3A were calibrated by incubating cells expressing each of these pH sensors in media with different pH values. Under well controlled metabolic conditions including the oxidative phosphorylation (OXPHOS) conditions in respiratory cells, the pH values at each of the pH sensors positions (MPP-sEcGFP, CoxVIIIa-sEcGFP, SU γ -sEcGFP, and SU e-sEcGFP) were ratiometrically determined according to the ratio of the measured emissions in the two channels ($\lambda_{511}/\lambda_{464}$).

Notably, based on the size of the sEcGFP⁴⁹ and its associated protein linker, the active site of its pH-sensitive chromophore is likely to be at least about 2–3 nm away from the mitochondrial crista membrane surface, which is perfect to measure bulk-liquid pH in the crista; but it is still too far away to detect TELP which typically stay within a 1-nm thin layer on the membrane surface. Therefore, according to the fundamental understanding with the TELP model (Fig. 2), we predict that the sEcGFP pH sensors including the MPP-sEcGFP, CoxVIIIa-sEcGFP, SU γ -sEcGFP, and SU e-sEcGFP as employed in the experiment of Rieger et al., 2021 (Fig. 3A) can see the protons in the bulk liquid phase, but none of them could detect TELP that stay within 1-nm thin layer on mitochondrial crista membrane surface.

The physical reason why TELP (transmembrane-electrostatically localized protons) stay within a 1-nm thin layer on membrane surface is because of the transmembrane attractive force between an excess proton on the *p*-side (of a typically 4-nm thin membrane) and an excess hydroxide on the *n*-side, which has been calculated to be as much as 1.92×10^{-11} N.²⁴ Consequently, to physically move a transmembrane-electrostatically localized proton away from the membrane surface by a nanometer (1 nm) towards the bulk liquid phase would require the work (*W*) of about 1.92×10^{-20} J (1.92×10^{-11} N \times 1.0×10^{-9} m) which is 4.5 times as much as the Boltzmann $k_B T$ thermal kinetic energy (4.28×10^{-21} J) at a physiological temperature of 37 °C (310 K).²⁴ Therefore, the excess protons-membrane-excess hydroxides capacitor system is so stable (TELP staying within its 1-nm thin layer) under the physiological temperature conditions that any pH sensor such as sEcGFP located at least about 2–3 nm away from the crista membrane surface will not be able to see TELP. This predicted feature as expected from the fundamental understanding with the TELP model (Fig. 2) was observed exactly in the experiment (Fig. 3) of Rieger et al., 2021.

As shown in Fig. 3B, under the OXPHOS (oxidative phosphorylation) conditions, the liquid pH values at the sites of CoxVIIIa-sEcGFP, SU γ -sEcGFP, SU e-sEcGFP, and MPP-sEcGFP were determined respectively to be 6.9, 7.3, 7.4, and 7.7. To an expert who really knows the field of protonic bioenergetics, these pH values obviously represent the mitochondrial bulk-liquid phase pH values but not TELP or “localized protons” although they were measured with the sEcGFP pH sensors near the membrane surface. However, it is also not too surprising for someone, especially those who may or may not fully understand the property of TELP, to believe these pH values as “local pH” or “localized protons”. For example, in a “critique”,⁴² Silverstein even took this type of pH values “6.8–7.0” (that were previously measured with sEcGFP pH sensors by the Rieger et al. team⁴) as “ pH_{surf} ” in arguing against the TELP theory^{5,8}; Obviously that “critique”⁴² was largely stemmed from some misunderstanding of the TELP theory.^{5,8}

Notably, all these sEcGFP-measured pH values “6.9, 7.3, 7.4, and 7.7” and “6.8–7.0” are in line with the mitochondrial bulk-liquid phase pH values (pH 7.35 in matrix liquid and pH 7.25 in intermembrane space/cristae liquid) measured independently by Chinopoulos et al. 2009.⁵⁰ Especially, the transmembrane bulk-liquid-phase pH difference (ΔpH) across the membrane-embedded ATP synthase (i.e., complex V

(CV)) for ATP synthesis, “CV (SU γ - SU e)”, was determined to be about 0.1 unit (= pH 7.4 – pH 7.3), which is in an excellent agreement with the independent experimental study of Chinopoulos et al. 2009⁵⁰ that demonstrated basically no or little bulk-phase pH difference between the matrix and the intermembrane space across the mitochondrial inner membrane: the “ ΔpH_{max} is only ~ 0.11 ”. Therefore, as predicted by the TELP model (Fig. 2), what the sEcGFP pH sensors detected at the sites of CoxVIIIa-sEcGFP and SU γ -sEcGFP was the intracristal liquid pH, but not the TELP activity (Fig. 3B).

2.3. Transmembrane potential $\Delta\psi$ indicating the presence of TELP in mitochondria

As illustrated in Fig. 2, under the oxidative phosphorylation conditions, excess protons are created on the intracristal side by the respiratory complexes I, III and IV that pump protons across the membrane from the extracristal side (matrix) while leaving excess hydroxides on the matrix side. The resulting formation of TELP (transmembrane-electrostatically localized protons) and their associated protonic capacitor have been mathematically justified through the application of the Gauss Law equation (Eq. 5) with liquid water as a protonic conductor. Furthermore, the formation of an “excess hydroxides-membrane-excess protons” capacitor and its associated TELP activity have recently been experimentally demonstrated using biomimetic “water-membrane-water” systems in the Lee laboratory.^{16–18,48}

The intimate relationship between the ideal TELP concentration $[H_T^+]^0$ and transmembrane potential difference $\Delta\psi$ is described in the TELP equation (Eq. 3), which shows that as long as there is a substantial value of $\Delta\psi$, there must be TELP; this relationship is true also for their vice versa. That is, TELP and $\Delta\psi$ represent the “two faces of a coin” like a photon’s “dual wave-particle behavior”. Here, if the “coin” represents a protonic capacitor, then TELP and $\Delta\psi$ represent its “two faces”. Fundamentally, it is the formation of a TELP-associated membrane capacitor that gives rise to $\Delta\psi$. On the other hand, the presence of $\Delta\psi$ must indicate the presence of TELP. In the experiment of Rieger et al., 2021, “the mitochondrial membrane potential, $\Delta\psi_m$, was determined using the membrane potential-sensitive dye TMRE (tetramethylrhodamine ethyl ester)”¹; Thus, the presence of mitochondrial membrane potential $\Delta\psi$ there was obvious, which clearly also indicates the presence of TELP.

As shown in Table 1, using Eqs. (3) and (4), the steady-state TELP surface density was calculated to be in a range from 3190 to 12800 excess protons per μm^2 of inner mitochondrial membrane surface area at the intracristal side when the transmembrane potential $\Delta\psi$ was in a range from 50 to 200 mV, respectively. At a typical transmembrane potential $\Delta\psi$ of 100 mV, the TELP surface density was calculated to be 6400 excess protons per μm^2 . A typical mitochondrion (in a size about 1500 nm \times 300 nm \times 300 nm with an ellipsoidal volume of about 5.65×10^8 nm³) has an inner membrane surface area of 5.76×10^6 nm². The TELP surface density of 6400 excess protons per μm^2 translates to a total of 37000 excess protons for a typical mitochondrion with inner membrane surface area of 5.76×10^6 nm² as reported previously.⁸

As illustrated in Figs. 2 and 3B, TELP as a protonic monolayer rightly over the protonic mouth of membrane-embedded F_0F_1 -ATP synthase can be a highly potent force in driving the synthesis of ATP. As shown in Table 1, the steady-state TELP surface density in a range from 3190 to 12800 excess protons per μm^2 translates to TELP-associated local pH (pH_{TELP}) at the liquid-membrane interface in a range from 2.27 to 1.67, respectively. This effective TELP-associated local pH (pH_{TELP}) ranging from 2.27 to 1.67 is equivalent to the effective TELP concentration ($[H_T^+]$) ranging from 5.30 to 21.2 mM which stays within the 1-nm thin layer at the liquid-membrane interface. That is, at a typical transmembrane potential $\Delta\psi$ of 100 mV, its TELP surface density of 6400 excess protons per μm^2 can translate to the TELP-associated local pH (pH_{TELP}) as low as about 2, which is equivalent to the effective TELP

Table 1

Mitochondrial protonic energetics and associated properties including the transmembrane-electrostatically localized protons (TELP) density per membrane surface area ($TELP$ per μm^2), TELP-associated local pH (pH_{TELP}) within its 1-nm thin layer at the liquid-membrane interface, TELP concentration ($[H_L^+]$) at the liquid-membrane interface, local protonic entropy change (ΔS_L), the classic protonic Gibbs free energy (ΔG_C), the local protonic Gibbs free energy (ΔG_L) and the total protonic Gibbs free energy (ΔG_T) calculated as a function of transmembrane potential $\Delta\psi$ using Eqs. (1)–(7) based on the measured properties (pH_{PB} , pH_{NB} , $\Delta\psi$) with the known reaction medium compositions of ref. 50 and the experimental measurements of pH across the membrane-embedded F_0F_1 -ATP synthase with the sEcGFP pH sensor fused to complex V subunit e and γ (CV SU e -sEcGFP and CV SU γ -sEcGFP) reported in Ref. 1. The cation concentrations, proton-cation exchange equilibrium constants and cation exchange reduction factor (1.29) are from Refs. 5,8; and the temperature $T = 310$ K. Adapted and updated from Ref. 57

$\Delta\psi$ mV	pH_{PB}	pH_{NB}	$TELP$ per μm^2	pH_{TELP}	$[H_L^+]$ mM	ΔS_L J/K.mol	ΔG_C kJ/mol	ΔG_L kJ/mol	ΔG_T kJ/mol	ΔG_{Syn} kJ/mol	ΔG_{Chem} kJ/mol
50	7.3	7.4	3190	2.27	5.30	-95.1	-5.42	-29.5	-34.9	-24.5	-22.0
55	7.3	7.4	3510	2.23	5.83	-95.9	-5.90	-29.7	-35.6	-24.5	-22.0
60	7.3	7.4	3830	2.19	6.36	-96.6	-6.38	-30.0	-36.3	-24.5	-22.0
65	7.3	7.4	4150	2.16	6.89	-97.3	-6.86	-30.2	-37.0	-24.5	-22.0
70	7.3	7.4	4470	2.13	7.42	-97.9	-7.35	-30.4	-37.7	-24.5	-22.0
75	7.3	7.4	4790	2.10	7.95	-98.5	-7.83	-30.5	-38.4	-24.5	-22.0
80	7.3	7.4	5110	2.07	8.48	-99.0	-8.31	-30.7	-39.0	-24.5	-22.0
90	7.3	7.4	5750	2.02	9.55	-100	-9.28	-31.0	-40.3	-24.5	-22.0
100	7.3	7.4	6390	1.97	10.6	-101	-10.2	-31.3	-41.5	-24.5	-22.0
110	7.3	7.4	7030	1.93	11.7	-102	-11.2	-31.5	-42.7	-24.5	-22.0
120	7.3	7.4	7660	1.90	12.7	-102	-12.2	-31.7	-43.9	-24.5	-22.0
130	7.3	7.4	8300	1.86	13.8	-103	-13.1	-31.9	-45.1	-24.5	-22.0
140	7.3	7.4	8940	1.82	14.8	-104	-14.1	-32.1	-46.2	-24.5	-22.0
150	7.3	7.4	9580	1.80	15.9	-104	-15.1	-32.3	-47.4	-24.5	-22.0
160	7.3	7.4	10200	1.77	17.0	-105	-16.0	-32.5	-48.5	-24.5	-22.0
170	7.3	7.4	10900	1.74	18.0	-105	-17.0	-32.6	-49.6	-24.5	-22.0
180	7.3	7.4	11500	1.72	19.1	-106	-18.0	-32.8	-50.7	-24.5	-22.0
190	7.3	7.4	12100	1.70	20.2	-106	-18.9	-32.9	-51.9	-24.5	-22.0
200	7.3	7.4	12800	1.67	21.2	-107	-19.9	-33.1	-52.9	-24.5	-22.0

concentration ($[H_L^+]$) of 10.6 mM (Table 1) that is quite powerful. Since TELP stays within the 1-nm thin layer on intracrystal membrane surface, it is not detectable to a sEcGFP pH sensor that was located at least 2–3 nm away from membrane surface. Therefore, the TELP property is highly special and powerful.

As discussed recently^{6,51}, the formation of TELP apparently represents a type of “negative entropy effect”^{48,51,52} that “brings the excess protons to the mouths of the pmf users (F_0F_1 -ATP synthase) where the protons can isothermally utilize their molecular thermal motions (protonic thermal kinetic energy $k_B T$) possibly including their random and chaotic Brownian motions to push through the doors of F_0F_1 -ATP synthase in driving ATP synthesis”. Consequently, despite the fact that the thermal energy-associated protonic translational motions (kinetic energy) are random and chaotic in all directions, “a localized proton at the water-membrane interface” has a much higher probability to chaotically hit through the mouth (F_0 protonic channel) of F_0F_1 -ATP synthase in driving the “ F_0 rotary molecular machinery for ATP synthesis” than “a delocalized proton in the bulk liquid phase that is far away from the protonic users”. Therefore, the protonic (TELP) thermal motion kinetic energy may be utilized to do useful work in driving ATP synthesis through F_0F_1 -ATP synthase, which as part of a thermotrophic function may convert a fraction of the thermal energy into the chemical energy of ATP. As shown in Eq. (2) “for the local pmf”, the thermotrophic function featured as “the utilization of protonic thermal kinetic energy $k_B T$ ” is essentially expressed as “ $RT (= k_B T \cdot N_A)$ which equals to the product of the Boltzmann constant k_B , the mitochondrial temperature T and the Avogadro constant N_A ”.

Bioenergetically, $\Delta\psi$ can be utilized to drive a charged particle such as proton through the protonic channel of F_0F_1 -ATP synthase across the membrane to do electric work ($e\Delta\psi$) in helping to drive ATP synthesis. In addition, TELP can utilize its thermal kinetic energy ($k_B T$) to hit through the protonic channel of F_0F_1 -ATP synthase in helping to drive ATP synthesis, which converts its environmental heat energy ($k_B T$) into the chemical energy locked into ATP molecules and thus represents a substantial thermotrophic feature.⁶ Therefore, both $\Delta\psi$ and TELP as “two sides of a coin” have their unique energetic roles with substantial biological significance.

2.4. TELP model better explaining the bioenergetics for oxidative phosphorylation in mitochondria

It is important to keep in mind the fundamental understanding of the TELP theory.^{5,8} For example, to some observers who may or may not have the full knowledge of the TELP theory, but experimentally observed the liquid pH 6.9 at CoxVIIIa-sEcGFP, pH 7.3 at SU γ -sEcGFP, pH 7.4 at SU e -sEcGFP, and pH 7.7 at SU e -sEcGFP, they (such as Rieger et al., 2021) could believe “The generated pH profiles revealed that the local Δp was unexpectedly low under OXPHOS, which are ATP synthesis conditions”.¹ Rieger et al., 2021 once concluded that “the Δp at ATP synthase is almost negligible under OXPHOS conditions”, stating “ATP synthesis is possible at low Δp ”. That conclusion of Rieger et al., 2021 shall now be revised according to the fundamental understanding of the TELP theory.^{5,8}

According to my analysis using the TELP model,^{5,8} with the transmembrane liquid-phase pH difference (ΔpH) of about 0.1 unit (= pH 7.4 – pH 7.3) across the membrane-embedded ATP synthase (complex V) as observed by Rieger et al., 2021, the energetics for ATP synthesis in mitochondria could not be explained by the classic Mitchellian protonic motive force (pmf) equation alone without considering the TELP activity. That is, the classic pmf value calculated with the classic Mitchellian pmf equation in the textbooks would not be sufficient to drive ATP synthesis, even if using the most conservatively estimated mitochondrial phosphorylation potential of -416 mV ($-9.6 \times 4.187 \div F$) as calculated from the Gibbs free energy change (ΔG_{ATP}) of $+9.6$ kcal/mol reported in Refs. 53–55 for ATP synthesis with a proton-to-ATP ratio of 8/3 (416 mV/2.67 = 156 mV).⁶ The proton-to-ATP ratio of 8/3 is consistent with the known structure of the animal mitochondrial F_0F_1 -ATP synthase, which has 3 catalytic sites for ATP synthesis, driven by a flow of 8 protons per revolution through the 8 c-subunits in its nanometer-scale molecular turbine ring.^{56–59}

Note, protonic motive force (pmf) is equivalent to Gibbs free energy ΔG in a simple relation with the Faraday constant (F) as shown in the following equation:

$$\Delta G = -F \times \text{pmf} \quad (6)$$

Therefore, the amount of total protonic Gibbs free energy (ΔG_T) may be calculated using the following equation:

$$\Delta G_T = -F\Delta\psi - 2.3 RT \log_{10} \left(\frac{[H_{pB}^+]}{[H_{nB}^+]} \right) - 2.3 RT \log_{10} \left(1 + \frac{[H_L^+]}{[H_{pB}^+]} \right) \quad (7)$$

where the first two terms represent the classic pmf free energy (ΔG_c) while the last term is the local pmf free energy (ΔG_L).

Furthermore, the phosphorylation potential (ΔG_{ATP}) for ATP synthesis employed by Slater⁵⁵ in his 1967 evaluation of the chemiosmotic hypothesis was +15.6 kcal/mol that had been experimentally determined by Cockrell et al. 1966⁵⁴ in isolated rat liver mitochondria. Notably, this phosphorylation potential of +15.6 kcal/mol (equivalent to 65.3 kJ mol⁻¹) for ATP synthesis is remarkably close to the magnitude of the critical free energy -63.5 kJ mol⁻¹ for ATP hydrolysis in an animal heart cell as measured by Wu et al. 2008⁶⁰ and thus it may be considered as a physiologically required phosphorylation potential (65.3 kJ mol⁻¹) for ATP synthesis. Based on this phosphorylation potential of +65.3 kJ mol⁻¹, the physiologically required protonic Gibbs free energy (ΔG_{Syn}) for ATP synthesis with a proton-to-ATP ratio of 8/3 in mitochondria should be -24.5 kJ mol⁻¹ (-65.3 kJ mol⁻¹/2.67).

Therefore, we have recently employed this phosphorylation potential (65.3 kJ mol⁻¹) to compare with the total protonic Gibbs free energy (ΔG_T) that consists of the classic pmf free energy (ΔG_c) and the local pmf free energy (ΔG_L) in mitochondria for ATP synthesis. Remarkably, the intracristae liquid pH 7.3 that Rieger et al., 2021 detected with SU γ -sEcGFP and the extracristal liquid pH 7.4 measured at SU e-sEcGFP are essentially the same as the transmembrane bulk-liquid pH values of “7.25” and “7.35” that we have recently used, respectfully, for the intracristae bulk-liquid phase pH_{pB} and the extracristal bulk-liquid phase pH_{nB} (Table 1,^{5,6,8}) across the membrane-embedded ATP synthase.

According to the data presented in Table 1 and Fig. 4, the classic protonic Gibbs free energy (ΔG_c in a range from -5.42 to -19.9 kJ mol⁻¹) alone is not adequate to explain the protonic energetics for ATP synthesis in mitochondria since the ΔG_c value is substantially below the

physiologically required protonic Gibbs free energy (ΔG_{Syn}) of -24.5 kJ mol⁻¹ for ATP synthesis at any point in the entire range of mitochondrial transmembrane potentials ($\Delta\psi$) from 50 to 200 mV. The *in vivo* mitochondrial transmembrane potential ($\Delta\psi$)^{61–63} values were experimentally observed to be mostly below 150 mV including 56 mV, 105 ± 0.9 mV, and 81 ± 0.7 mV measured by Zhang et al. (2001),⁶⁴ 91 ± 11 mV and 81 ± 13 mV determined by Gurm et al. (2012) using the techniques of 4-18Ffluorophenyltriphenylphosphonium and *in vivo* positron emission tomography (PET) measurement,⁶⁵ and also 114 mV and 123 mV reported in swine and human respectfully using an improved PET-based method by Alpert et al. 2018⁶¹ and by Pelletier-Galarneau et al. 2020.⁶⁶ We recently reported^{6,7} that the classic Mitchellian chemiosmotic theory^{67–69} cannot explain the mitochondrial energetics in living cells because it fatally misses to account for the TELP Gibbs free energy contribution in mitochondria.^{5,8,51}

These findings are well corroborated with the mysterious problem previously commented by Silverstein (2014) as a “thermodynamic efficiency of 113%” in mitochondria at a transmembrane potential of around 80 mV.⁵³ According to the classic Mitchellian pmf equation,^{67,70,71} to avoid the “impossibly high efficiency (>100%)” for mitochondria, one would have to “adjust” the bulk-phase “ ΔpH (in-out)” to an arbitrary value of at least “+2.5”. However, as mentioned above, the experiment of Rieger et al., 2021 using the calibrated ratiometric sEcGFP pH sensors clearly confirmed that the transmembrane bulk-liquid-phase pH difference (ΔpH) is only 0.1 unit (= pH 7.4 - pH 7.3) across the membrane-embedded ATP synthase (complex V). This sEcGFP experimental observation of transmembrane liquid-phase pH difference (ΔpH) of 0.1 unit is well in line with previously reported independent observations that the bulk-phase ΔpH (in-out) is nearly zero: “ ΔpH_{max} is only ~0.11” based on the modern experimental measurements⁵⁰ and modeling analysis of mitochondria.⁷² The observed bulk-phase ΔpH of nearly zero in mitochondria⁵⁰ is also corroborated with the prediction from the TELP theory^{5,8,28,48,52} with the

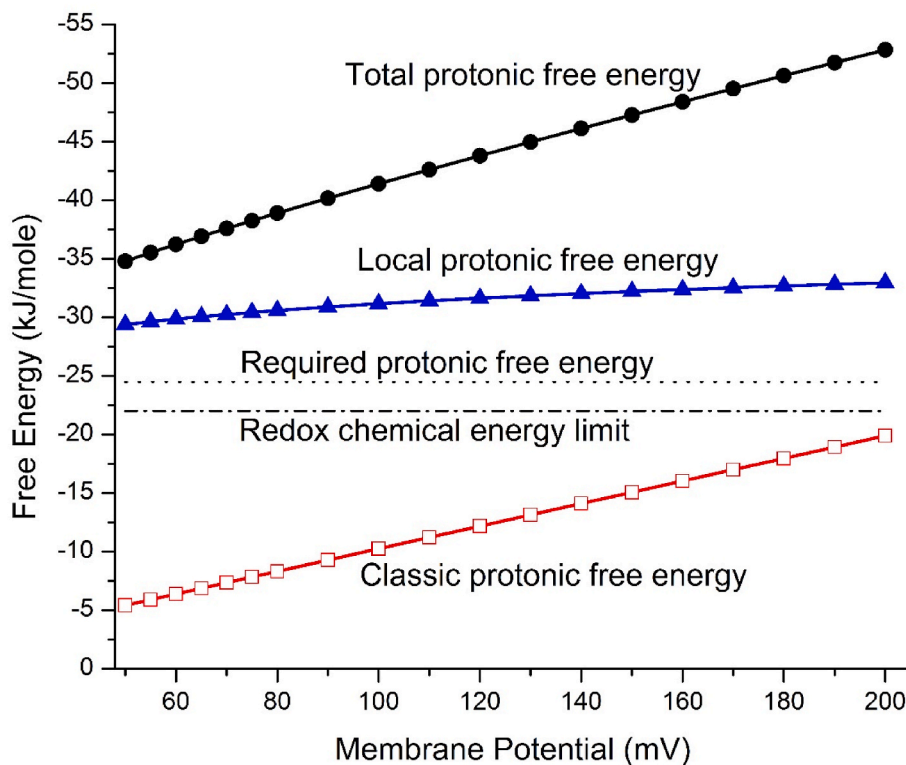


Fig. 4. Gibbs free energy (ΔG) values including the total protonic Gibbs free energy (ΔG_T), local protonic Gibbs free energy (ΔG_L), and classic protonic Gibbs free energy (ΔG_c) in mitochondria calculated as a function of transmembrane potential $\Delta\psi$ compared to the required protonic Gibbs free energy of -24.5 kJ mol⁻¹ for ATP synthesis (ΔG_{Syn}) and to the redox potential chemical energy upper limit (ΔG_{chem}) of -22.0 kJ mol⁻¹. Adapted from Ref. 7.

understanding that mitochondrial inner membrane is rather impermeable to ions.^{73,74} An independent study using a pH-sensitive GFP⁷⁵ has now also showed “that the intracristae lumen does not provide a reservoir for substrate protons for ATP synthesis” indicating “kinetic coupling of the respiratory chain with ATP synthase, but not proton gradients, drives ATP production in cristae membranes”. Therefore, it is now quite clear that the classic Mitchellian chemiosmotic theory^{67–69} alone cannot explain the energetics in mitochondria; there must be another rather disparate protonic energetics mechanism in driving the synthesis of ATP through the F₀F₁-ATP synthase.

We now understand, this disparate protonic energetics mechanism acts through the local protonic Gibbs free energy (ΔG_L) from TELP.^{5,8–11,28,51,52} As shown in Table 1 and Fig. 4, the calculated local protonic Gibbs free energy (ΔG_L) is in a range from -29.5 to -33.1 kJ mol⁻¹ whereas the classic protonic Gibbs free energy (ΔG_C) is in a range from -5.42 to -19.9 kJ mol⁻¹ for a range of transmembrane potential ($\Delta\psi$) from 50 to 200 mV. The total protonic Gibbs free energy (ΔG_T) that is the sum of the classic protonic Gibbs free energy (ΔG_C) and the local protonic Gibbs free energy (ΔG_L) was calculated to be in a range from -34.9 to -52.9 kJ mol⁻¹. All of these ΔG_L and ΔG_T values (Table 1) are substantially above the physiologically required ΔG_{Syn} of -24.5 kJ mol⁻¹ for ATP synthesis at any of the transmembrane potential ($\Delta\psi$) values in a range from 50 to 200 mV. Therefore, the application of the newly formulated protonic Gibbs free energy equations (Eqs. (1)–(7)) has now consistently yielded an excellent elucidation for the energetics in mitochondria, which does not require any arbitrary adjustment in the number of the bulk-phase “ Δ pH (in-out)” that the previous study⁵³ had to require.

The redox potential chemical energy upper limit (ΔG_{Chem}) for the entire respiratory redox-driven proton pump system in mitochondria was calculated to be about -22.0 kJ mol⁻¹ as follows. The redox potential difference between the electron donor NADH ($E_{m,7} = -320$ mV) to the terminal electron acceptor O₂ ($E_{m,7} = +820$ mV) in this system is known to be about 1140 mV.²² For each pair of electrons from NADH to pass through the respiratory chain (complexes I, III and IV) to the terminal electron acceptor O₂ as shown in Fig. 2, the system drives the translocation of 10 protons across the membrane from the matrix to the intermembrane space/crista space.⁸ That is, it couples the translocation of 5 protons per electron transport. Therefore, the maximum pmf that could be generated by the redox-driven proton pump system should be about 228 mV per proton (1140 mV/5 protons), equivalent to -22.0 kJ mol⁻¹ ($= -F \times 228$ mV) as the redox potential chemical energy limit (ΔG_{Chem}).

Notably, even the redox potential chemical energy limit ΔG_{Chem} which represents the theoretical chemical energy upper limit (-22.0 kJ mol⁻¹) of the classic Mitchellian bulk phase-to-bulk phase protonic electrochemical potential gradients,^{67–69} is still below the physiologically required ΔG_{Syn} of -24.5 kJ mol⁻¹ for ATP synthesis in mitochondria. Therefore, the known classic chemical energy process alone is not adequate to explain the protonic energetics in mitochondria. This also indicates that there must be another fundamentally disparate biophysical energetics mechanism in mitochondria; which we now know is the thermotrophic function^{6,33,34,35,36} isothermally utilizing environmental heat energy associated with TELP in driving the synthesis of ATP molecules.

As listed in Table 1, the entropy change (ΔS_L) for the TELP-associated isothermal environmental heat utilization process is indeed a negative number in a range from -95.1 to -107 J per Kelvin per mole (J/K.mol) when the TELP concentration [H_L^+] is in a range from 5.30 to 21.2 mM, which is a function of the transmembrane potential ($\Delta\psi$) in a range from 50 to 200 mV. This is a significant result (Table 1) since it has now numerically shown that the TELP membrane capacitor formation indeed represents a negative entropy event.

The calculated total protonic Gibbs free energy (ΔG_T) data including the local protonic Gibbs free energy (ΔG_L) (Table 1 and Fig. 4) showed a

plenty of protonic Gibbs free energy well above the ΔG_{Syn} of -24.5 kJ mol⁻¹ for ATP synthesis through the mitochondrial F₀F₁-ATP synthase even at a relatively low transmembrane potential ($\Delta\psi$) level anywhere in the range from about 50 mV to 200 mV. This finding is remarkably in line with the independent experimental observations of mitochondrial transmembrane potentials ($\Delta\psi$) in living cells being mostly about 56 mV, 105 ± 0.9 mV and 81 ± 0.7 mV,⁶⁴ 91 ± 11 mV and 81 ± 13 mV,⁶⁵ and also 114 mV⁶¹ and 123 mV⁶⁶ where apparently substantial amounts of ATP are synthesized at such relatively low mitochondrial transmembrane potentials to sustain the growth and activities of the living cells.

These results all show that when the TELP activity is included (Table 1, Figs. 2, 3B and 4) using newly formulated protonic bioenergetics equations (Eqs. (1)–(7)), there is plenty of total protonic Gibbs free energy (ΔG_T) that is well above the physiologically required protonic Gibbs free energy (ΔG_{Syn}) of -24.5 kJ mol⁻¹ to drive ATP synthesis through the F₀F₁-ATP synthase in mitochondria. Therefore, the previously reported conclusion “the Δ p at ATP synthase is almost negligible under OXPHOS conditions” of Rieger et al., 2021 shall now be revised and updated with the fundamental understanding of the TELP theory.^{5,8} That is, there actually is sufficient amount of total transmembrane protonic motive force gradient “ Δ p at ATP synthase” when the TELP activity is included in the protonic energy calculation with the fundamental understanding of the TELP model (Eqs. (1)–(7)).

2.5. The Mitchellian classic protonic motive force also at play in mitochondria

Although TELP activity appears as the dominant protonic motive force in driving ATP synthesis through F₀F₁-ATP synthase in mitochondria, it is worthwhile to note that the Mitchellian classic protonic motive force is also at play here as shown in Table 1 and Fig. 4. For example, at a mitochondrial transmembrane potential $\Delta\psi$ of 100 mV, classic protonic Gibbs free energy (ΔG_C) is -10.2 kJ mol⁻¹ (equivalent to pmf of 106 mV) although it is substantially smaller than the TELP-associated local pmf free energy (ΔG_L) of -31.3 kJ mol⁻¹ (equivalent to pmf of 324 mV) in their absolute values. Therefore, the Mitchellian classic protonic motive force Gibbs free energy is still also at play in mitochondrial energetics although the TELP-associated local protonic free energy (ΔG_L) appears to be the major driving force for ATP synthesis through F₀F₁-ATP synthase.

Furthermore, as calculated from the second term of the newly formulated total protonic Gibbs free energy (ΔG_T) equation (Eq. 7) (equivalent to the second term of Eq. (1)), -0.59 kJ mol⁻¹ (equivalent to pmf of 6.1 mV) of the classic protonic Gibbs free energy (ΔG_C) is contributed by the transmembrane bulk-liquid-phase pH difference (Δ pH) of 0.1 unit ($= \text{pH } 7.4 - \text{pH } 7.3$) experimentally confirmed by Rieger et al., 2021 across the membrane-embedded F₀F₁-ATP synthase. Although the free energy contribution (-0.59 kJ mol⁻¹) from the transmembrane bulk-liquid-phase pH difference (Δ pH) of 0.1 unit appears to be small in comparing to that of TELP free energy (ΔG_L) of -31.3 kJ mol⁻¹, one shall still pay attention not to neglect its scientific significance since it technically also indicates that the “Mitchellian bulk phase-to-bulk phase proton electrochemical potential gradients” is still part of the protonic energetic processes in mitochondria.

As calculated through the cation-proton exchange equation (Eq. 4) with the mitochondrial cation exchange reduction factor of 1.29 reported previously,^{5,8} a small fraction (22% = $1 - 1/1.29$) of the ideal TELP population can be exchanged out of the TELP layer into the bulk-liquid phase, resulting in a slightly lower pH in the intracristal liquid. Therefore, based on the fundamental understanding of the TELP theory with the cation-proton exchange equation (Eq. 4) and with the newly formulated total protonic Gibbs free energy (ΔG_T) equation (Eq. 7), there can be some bulk-liquid-phase protonic conduction from the protonic sources to the protonic users as well. This may manifest as a

lateral intracristal liquid pH gradient from the active protonic pumps (the supercomplexes of CI, CIII and CIV) at the relatively flat region of a crista to the ATP synthase dimer at the tip of the crista, in addition to the dominant TELP translocation pathway along the intracristal membrane surface at the steady state under OXPHOS conditions (Fig. 2). Likewise, we can also predict that there could be a liquid pH gradient from the protonic outlet of F_0F_1 -ATP synthase to the matrix bulk liquid phase that connects with the protonic pump inlets of the respiratory complexes I, III and IV in forming a complete protonic circuit. These features as predicted from the fundamental understanding of the TELP theory were exactly observed in the experiment of Rieger et al., 2021 as shown in Fig. 3B: 1) the lateral intracristal liquid pH gradient from the liquid pH 6.9 sensed by a sEcGFP linked at the Cox8a of CIV in the intracristal space to the intracristal liquid pH 7.3 measured with a sEcGFP linked at the *p*-side subunit *e* of F_0F_1 -ATP synthase; and 2) pH gradient from the liquid pH 7.4 measured with a sEcGFP linked at the *n*-side subunit *y* of F_0F_1 -ATP synthase to the liquid pH 7.7 detected with MPP-sEcGFP in the matrix.

The “radial pH gradient” from liquid pH 7.4 measured with a sEcGFP linked at the *n*-side subunit *y* of F_0F_1 -ATP synthase to the liquid pH 7.7 detected in the matrix with MPP-sEcGFP may be explained by the steady-state emerging protons from the *n*-side protonic outlet of F_0F_1 -ATP synthase to disperse into the pH 7.7 matrix liquid that is connected with protonic pump inlets of the respiratory complexes I, III and IV.

Therefore, the experimental observations of Rieger et al., 2021 using sEcGFP pH sensors at spatially discrete points in the intracristal liquid and extracristal liquid are highly valuable since they not only confirmed the transmembrane liquid-phase pH difference (ΔpH) of 0.1 unit (= pH 7.4 – pH 7.3) across the membrane-embedded F_0F_1 -ATP synthase but also showed the involvement of “Mitchellian bulk phase-to-bulk phase proton electrochemical potential gradients” with steady-state lateral liquid pH gradient along the intracristal space and a radial pH gradient from *n*-side subunit *y* of F_0F_1 -ATP synthase towards the matrix (Fig. 3B). This is in line with the understanding that about 20% of TELP formed from the protons pumped across the inner mitochondrial membrane may enter the intracristal bulk liquid through the cation-proton exchange process (Eq. (4)); they can then go through the intracristal bulk liquid phase to the protonic users located at the cristal rim, although TELP conducting along the intracristal membrane surface to the protonic users (F_0F_1 -ATP synthase dimer) at the cristal tip appears to be the major driving force for ATP synthesis under OXPHOS conditions.

Likewise, under the “glycolytic conditions” where the F_0F_1 -ATP synthase runs in reverse pumping protons into the intracristal space through ATP hydrolysis, we can predict that the pH at subunit (SU) *e* (of F_0F_1 -ATP synthase) will slightly decrease because a small fraction of the reversely pumped protons will also go to the intracristal liquid phase. Meanwhile, the pH at Cox8a (of CIV) will slightly increase because of limited respiratory-driven proton pump activity there under the glycolytic conditions. These features as predicted from the fundamental understanding of the TELP model were observed also exactly in the experiment of Rieger et al., 2021 that showed pH 7.1 at SU *e* of ATP synthase and pH 7.2 at subunit CoxVIIIa of CIV.¹

All these also show that the TELP theory^{5,8–11,28,51,52} may represent a complementary development to Mitchell’s chemiosmotic theory.^{20,21} The combination of the two together as expressed in Eqs. (1)–(7) can now well explain the energetics in mitochondria.

2.6. Additional explanations possible for the observed lateral intracristal liquid pH gradient

Therefore, with the fundamental understanding of the TELP model, we have now successfully explained all the major experimental observations of Rieger et al., 2021. However, it is worthwhile to note that additional and/or alternative explanations may also be possible for the lateral intracristal liquid pH gradient observed by Rieger et al., 2021. One of the questions is whether this observation could be explained by

the possibility that TELP and bulk-liquid protons (pH) do not show a sharp edge, at least not at protein surfaces. This possibility is quite unlikely since the transmembrane attractive force between an excess proton on the *p*-side (of a typically 4-nm thin membrane) and an excess hydroxide on the *n*-side is so strong as to physically move a transmembrane-electrostatically localized proton away from the membrane surface by a nanometer (1 nm) towards the bulk liquid phase would require a work (*W*) of 4.5 times as much as the Boltzmann $k_B T$ thermal kinetic energy (4.28×10^{-21} J) at the physiological temperature of 37 °C (310 K).²⁴ In this case, the possibility of finding TELP outside its 1-nm thin layer should be practically zero.

Another question is whether the sEcGFP pH sensor of Rieger et al., 2021 is measuring between membrane surface and bulk-liquid pH. Based on the property of TELP staying within the 1-nm thin layer on membrane surface, the sEcGFP-measured pH values are most likely to represent the bulk-liquid pH.

Yet, another question is whether the lateral TELP electrostatic distribution gradient that I previously identified⁸ could somehow effect a lateral intracristal liquid pH gradient like the one observed by Rieger et al., 2021. As shown in Fig. 2, my previous study showed that the lateral asymmetric feature resulted from the geometric effect of a crista can enhance the density of TELP at the crista tip where the F_0F_1 -ATP synthase enzymes are located by a factor of the axial ratio (*a/b*) for an ellipsoidal-shaped mitochondrial crista (Fig. 2). The TELP density at a crista tip can be as much as 10 times (1 pH unit) higher than that of the relatively flat membrane region where the proton pumping complexes I, III and IV are located.⁸ This finding was in line with an independent study⁷⁶ that proposed “a significant increase in charge density, and thus in the local pH gradient of ~0.5 units in regions of high membrane curvature”. Therefore, a question is whether this type of lateral TELP density gradient along the intracristal membrane surface can somehow also result in the formation of a lateral intracristal bulk-liquid pH gradient. Currently, that is not yet understood. It is prudent to keep this type of question in mind for future research effort.

3. Conclusion

Rieger et al., 2021 performed a wonderful pH-sensing GFP experimental study using the radiometric sEcGFP in mitochondria of live cells, where “pH profiles of mitochondrial sub-compartments were recorded with high spatial resolution in live mammalian cells by positioning a pH sensor directly at ATP synthase’s F_1 and F_0 subunits, complex IV and in the matrix”. They elegantly measured the intracristal liquid pH to be 7.3 using the SU γ -sEcGFP at the *p*-side and the extracristal liquid pH to be 7.4 with SU ϵ -sEcGFP at the *n*-side of the membrane-embedded F_0F_1 -ATP synthase. Remarkably, both the intracristal liquid pH 7.3 and extracristal liquid pH 7.4 as measured with sEcGFP at the two sides of the membrane-embedded F_0F_1 -ATP synthase were in excellent agreement with the intracristal bulk-liquid phase pH_{pB} of “7.25” and the extracristal bulk-liquid phase pH_{nB} of “7.35” that were employed in our published mitochondrial energetics studies.^{5–7}

In the experiment of Rieger et al., 2021, “the mitochondrial membrane potential, $\Delta\psi_m$, was determined using the membrane potential-sensitive dye TMRE” and the presence of mitochondrial membrane potential $\Delta\psi$ was obvious, which clearly indicates the presence of TELP as shown in the protonic capacitor-based TELP equation (Eq. 3).

Under the oxidative phosphorylation (OXPHOS) conditions, the formation of a protonic capacitor across a crista membrane is now mathematically justified by using the Gauss law equation (Eq. 5). In the protonic membrane capacitor, the physical reason why TELP stays within its 1-nm thin layer on membrane surface is because of the transmembrane attractive force between an excess proton on the *p*-side (of a typically 4-nm thin membrane) and an excess hydroxide on the *n*-side, which has been calculated to be as much as 1.92×10^{-11} N.²⁴ Consequently, to physically move a transmembrane-electrostatically localized proton away from the membrane surface by a nanometer (1

nm) towards the bulk liquid phase would require the work (W) of about 1.92×10^{-20} J, which is 4.5 times as much as the Boltzmann $k_B T$ thermal kinetic energy (4.28×10^{-21} J) at the physiological temperature of 37 °C.²⁴ This explains how TELP stays within 1-nm thin layer under the physiological temperature conditions so that any pH sensor outside of the 1-nm thin TELP layer such as the sEcGFP pH sensors located at least 2–3 nm away from the membrane surface will not be able to see TELP activity. This feature as predicted from the fundamental understanding with the TELP model (Fig. 2) was observed exactly in the experiment (Fig. 3) of Rieger et al., 2021.

To some observers such as Rieger et al., 2021 who experimentally observed the liquid pH 6.9 at CoxVIIIa-sEcGFP, pH 7.3 at SU γ -sEcGFP, pH 7.4 at SU e-sEcGFP, and pH 7.7 at SU e-sEcGFP, but who may or may not be fully aware of the TELP theory,^{5,8} it would not be surprising for them (including Rieger et al., 2021) to believe “the Δp at ATP synthase is almost negligible under OXPHOS conditions”. In contrast, I find, when the TELP activity is included in the energy calculations using the newly formulated protonic bioenergetics equations (Eqs. (1)–(7)), it shows plenty of total protonic Gibbs free energy (ΔG_T) that is well above the physiologically required protonic Gibbs free energy (ΔG_{Syn}) of -24.5 kJ mol⁻¹ to drive ATP synthesis through the F₀F₁-ATP synthase in mitochondria at any of the transmembrane potential values in the entire range from 50 to 200 mV (Table 1, Fig. 4).

This study also shows that the TELP theory^{5,8–11,28,51,52} may represent a complementary development to Mitchell’s chemiosmotic theory.^{20,21} The combination of the two together as expressed in Eqs. (1)–(7) can now excellently explain the energetics in mitochondria. Consequently, the experimental observations of Rieger et al., 2021 under the OXPHOS conditions is now better elucidated with a protonic capacitor concept in accordance with the fundamentals of the TELP model,^{5,8} which is fundamentally important to the science of bioenergetics.

Funding declaration

The protonic bioenergetics aspect of this research was supported in part by a Multidisciplinary Biomedical Research Seed Funding Grant from the Graduate School, the College of Sciences, and the Center for Bioelectrics at Old Dominion University, Norfolk, Virginia, USA.

Ethics approval

This research does not involve any clinical research.

Data availability

All data generated or analyzed during this study are included in this article and in the cited references.

Consent to participate

This research does not involve any clinical research.

Credit authorship contribution statement

James Weifu Lee: designed and performed research, analyzed data, and authored the paper.

Declaration of competing interest

The author declares no competing financial and non-financial interests.

Acknowledgement

The author thanks Prof. Karin B. Busch of Germany for the discussions on her team’s wonderful pH-sensing GFP mitochondrial

experimental results (Rieger et al., 2014 and 2021) and for her highly valuable suggestions and review feedback that made this manuscript better. The author also thanks the anonymous peer reviewers for their highly valuable and constructive review comments that also made this article better. The author also thanks for the support provided in part by the Multidisciplinary Biomedical Research Seed Funding Grant from the Graduate School, the College of Sciences, and the Center for Bioelectrics at Old Dominion University, Norfolk, Virginia, USA.

References

- Rieger B, Arroum T, Borowski M-T, Villalta J, Busch KB. Mitochondrial FIFO ATP synthase determines the local proton motive force at cristae rims. *EMBO Rep.* 2021; 22, e52727. <https://doi.org/10.15252/embr.202152727>.
- Orij R, Postmus J, Ter Beek A, Brul S, Smits GJ. In vivo measurement of cytosolic and mitochondrial pH using a pH-sensitive GFP derivative in *Saccharomyces cerevisiae* reveals a relation between intracellular pH and growth. *Microbiol-Sgm.* 2009;155: 268–278. <https://doi.org/10.1099/mic.0.022038-0>.
- Gao DJ, Knight MR, Trewas AJ, Sattelmacher B, Plieth C. Self-reporting arabidopsis expressing pH and [Ca²⁺] indicators unveil ion dynamics in the cytoplasm and in the apoplast under abiotic stress. *Plant Physiol.* 2004;134:898–908. <https://doi.org/10.1104/pp.103.032508>.
- Rieger B, Junge W, Busch KB. Lateral pH gradient between OXPHOS complex IV and FOF1 ATP-synthase in folded mitochondrial membranes. *Nat Commun.* 2014;5. <https://doi.org/10.1038/ncomms4103>. ARTN 3103.
- Lee JW. Electrostatically localized proton bioenergetics: better understanding membrane potential. *Heliyon.* 2019;5, e01961. <https://doi.org/10.1016/j.heliyon.2019.e01961>.
- Lee JW. Mitochondrial energetics with transmembrane electrostatically localized protons: do we have a thermotrophic feature? *Sci Rep-UK.* 2021;11. <https://doi.org/10.1038/s41598-021-93853-x>. ARTN 14575.
- Lee JW. Energy renewal: isothermal utilization of environmental heat energy with asymmetric structures. *Entropy-Switz.* 2021;23:665.
- Lee JW. Protonic Capacitor: elucidating the biological significance of mitochondrial cristae formation. *Nat Res J: Sci Rep.* 2020;10, 10304. <https://doi.org/10.1038/s41598-020-66203-6>.
- Lee JW. A possible electrostatic interpretation for proton localization and delocalization in chloroplast bioenergetics system. *Biophys J.* 2005;88:324a–325a.
- Lee JW. Proton-electrostatics hypothesis for localized proton coupling bioenergetics. *Bioenergetics.* 2012;1(104):1–8. <https://doi.org/10.4172/2167-7662.1000104>.
- Lee JW. Electrostatically localized protons bioenergetics over Mitchell’s classic chemiosmotic theory. *Biochem. Mol. Eng.* 2013;2:4. <https://doi.org/10.4172/2161-1009.S1.002>.
- de Grothuss CJT. Sur la décomposition de l’eau et des corps qu’elle tient en dissolution à l’aide de l’électricité galvanique. *Ann Chim.* 1806;58:54–73.
- Marx D, Tuckerman ME, Hutter J, Parrinello M. The nature of the hydrated excess proton in water. *Nature.* 1999;397:601–604.
- Pomès R, Roux B. Molecular mechanism of H⁺ conduction in the single-file water chain of the gramicidin channel. *Biophys J.* 2002;82:2304–2316.
- Marx D. Proton transfer 200 years after von Grothuss: insights from ab initio simulations. *ChemPhysChem.* 2006;7:1848–1870.
- Saeed HA, Lee JW. Experimental demonstration of localized excess protons at a water-membrane interface. *Bioenergetics.* 2015;4(127):1–7. <https://doi.org/10.4172/2167-7662.1000127>.
- Saeed H. *Bioenergetics: Experimental Demonstration of Excess Protons and Related Features.* Norfolk, VA 23529 USA: Old Dominion University; 2016. PhD Thesis.
- Saeed H, Lee J. Experimental determination of proton-cation exchange equilibrium constants at water-membrane interface fundamental to bioenergetics. *WATER J: Multidiscip Res J.* 2018;9:116–140. <https://doi.org/10.14294/WATER.2018.2>.
- Saeed HA, Lee JW. Experimental demonstration of localized excess protons at a water-membrane interface and the effect of other cations on their stability. *Faseb J.* 2016;30.
- Mitchell P, Moyle J. Estimation of membrane potential and Ph difference across cristae membrane of rat liver mitochondria. *Eur J Biochem.* 1969;7:471. &.
- Mitchell P. The correlation of chemical and osmotic forces in biochemistry. *J Biochem.* 1985;97:1–18.
- Nicholls DG, Ferguson SJ. 3 - quantitative bioenergetics: the measurement of driving forces. In: *Bioenergetics.* fourth ed. Academic Press; 2013:27–51. <https://doi.org/10.1016/B978-0-12-388425-1.00003-8>.
- Nicholls DG, Ferguson SJ. 3 - quantitative bioenergetics: the measurement of driving forces. In: Ferguson DGNJ, ed. *Bioenergetics.* 2. Academic Press; 1992:38–63. <https://doi.org/10.1016/B978-0-12-518124-2.50008-4>.
- Lee JW. Protonic conductor: better understanding neural resting and action potential. *J Neurophysiol.* 2020;124:1029–1044. <https://doi.org/10.1152/jn.00281.2020>.
- Guffanti A, Krulwich T. Bioenergetic problems of alkaliphilic bacteria. *Biochem Soc Trans.* 1984;12:411.
- Krulwich TA, Gilmour R, Hicks DB, Guffanti AA, Ito M. Energetics of alkaliphilic *Bacillus* species: physiology and molecules. *Adv Microb Physiol.* 1998;40:401–438.
- Krulwich TA, Liu J, Morino M, Fujisawa M, Ito M, Hicks DB. Adaptive mechanisms of extreme alkaliphiles. *Extremophiles Handb.* 2011:119–139.

- 28 Lee JW. Proton-electrostatic localization: explaining the bioenergetic conundrum in alkalophilic bacteria. *Bioenergetics*. 2015;4(121):1–8. <https://doi.org/10.4172/2167-7662.1000121>.
- 29 Lee JW. *Localized Excess Protons and Methods of Making and Using the Same*. PCT International Patent Application Publication No; 2017:56. WO 2017/007762 A1.
- 30 Lee JW. Physical chemistry of living systems: isothermal utilization of latent heat by electrostatically localized protons at liquid-membrane interface. *Biophys J*. 2019;116:317a. <https://doi.org/10.1016/j.bpj.2018.11.1719>.
- 31 Lee JW. Proton motive force computation revealing latent heat utilization by electrostatically localized protons at a liquid-biomembrane interface. *Abstr Pap Am Chem Soc*. 2018; 255.
- 32 Lee JW. Elucidating the 30-year-longstanding bioenergetic mystery in alkalophilic bacteria. *Biophys J*. 2017;112:278a–279a. <https://doi.org/10.1016/j.bpj.2016.11.1509>.
- 33 Lee JW. Isothermal environmental heat energy utilization by transmembrane electrostatically localized protons at the liquid-membrane interface. *ACS Omega*. 2020;5:17385–17395. <https://doi.org/10.1021/acsomega.0c01768>.
- 34 Lee JW. Type-B energy process: asymmetric function-gated isothermal electricity production. *Energies*. 2022;15:7020.
- 35 Lee JW. Type-B energetic processes and their associated scientific implication. *J Sci Explor*. 2022;36:487–495. <https://doi.org/10.31275/20222517>.
- 36 Lee JW. Thermotrophy exploratory study. *J Sci Explor*. 2023;37:5–16. <https://doi.org/10.31275/20232655>.
- 37 Sheehan DP, Moddel G, Lee JW. More on the demons of thermodynamics. *Phys Today*. 2023;76. <https://doi.org/10.1063/Pt.3.5186>, 13-13.
- 38 Guan L. Structure and mechanism of membrane transporters. *Sci Rep-Uk*. 2022;12, 13248. <https://doi.org/10.1038/s41598-022-17524-1>.
- 39 Zhang C, Knyazev DG, Vereshaga YA, et al. Water at hydrophobic interfaces delays proton surface-to-bulk transfer and provides a pathway for lateral proton diffusion. *P Natl Acad Sci USA*. 2012;109:9744–9749. <https://doi.org/10.1073/pnas.1121227109>.
- 40 Cherepanov DA, Feniouk BA, Junge W, Mulikidjanian AY. Low dielectric permittivity of water at the membrane interface: effect on the energy coupling mechanism in biological membranes. *Biophys J*. 2003;85:1307–1316. [https://doi.org/10.1016/S0006-3495\(03\)74565-2](https://doi.org/10.1016/S0006-3495(03)74565-2).
- 41 Mulikidjanian AY, Heberle J, Cherepanov DA. Protons @ interfaces: implications for biological energy conversion. *Bba-Bioenergetics*. 2006;1757:913–930. <https://doi.org/10.1016/j.bbabi.2006.02.015>.
- 42 Silverstein TP. A critique of the capacitor-based "transmembrane electrostatically localized proton" hypothesis. *J Bioenerg Biomembr*. 2022;54:59–65. <https://doi.org/10.1007/s10863-022-09931-w>.
- 43 Silverstein TP. The proton in biochemistry: impacts on bioenergetics, biophysical chemistry, and bioorganic chemistry. *Front Mol Biosci*. 2021;8. <https://doi.org/10.3389/fmolb.2021.764099>. ARTN 764099.
- 44 Lee JW. Protonic conductor: explaining the transient "excess protons" experiment of Pohl's group 2012. *Biophys Chem*. 2023, 106983. <https://doi.org/10.1016/j.bpc.2023.106983>.
- 45 Agmon N, Gutman M. Proton fronts on membranes. *Nat Chem*. 2011;3:840–842. <https://doi.org/10.1038/nchem.1184>.
- 46 Lee JW. Transient protonic capacitor: explaining the bacteriorhodopsin membrane experiment of Heberle et al. 1994. *Biophys Chem*. 2023, 107072. <https://doi.org/10.1016/j.bpc.2023.107072>.
- 47 Ohanian HC. Gauss' law. In: *Physics*. W. W. Norton & Company; 1985:565–573.
- 48 Lee JW. *Localized Excess Protons and Methods of Making and Using the Same*. A1. United States Patent Application Publication No. US 20170009357; 2017:73pp.
- 49 Rieger B, Shalaeva DN, Sohnel AC, et al. Lifetime imaging of GFP at CoxVIII reports respiratory supercomplex assembly in live cells. *Sci Rep-Uk*. 2017;7. <https://doi.org/10.1038/srep46055>. ARTN 46055.
- 50 Chinopoulos C, Vajda S, Csanady L, Mandi M, Mathe K, Adam-Vizi V. A novel kinetic assay of mitochondrial ATP-ADP exchange rate mediated by the ANT. *Biophys J*. 2009;96:2490–2504. <https://doi.org/10.1016/j.bpj.2008.12.3915>.
- 51 Lee JW. Isothermal environmental heat energy utilization by transmembrane electrostatically localized protons at the liquid-membrane interface. *ACS J Omega*. 2020. <https://doi.org/10.1021/acsomega.0c01768>.
- 52 Lee, J.W. (2019) Localized excess protons and methods of making and using same. USA patent US 10,501,854 B2, patent application 15/202,214, and granted 2018/12/10..
- 53 Silverstein TP. An exploration of how the thermodynamic efficiency of bioenergetic membrane systems varies with c-subunit stoichiometry of F1F0 ATP synthases. *J Bioenerg Biomembr*. 2014;46:229–241. <https://doi.org/10.1007/s10863-014-9547-y>.
- 54 Cockrell RS, Harris EJ, Pressman BC. Energetics of potassium transport in mitochondria induced by Valinomycin. *Biochemistry-U.S.* 1966;5:2326. <https://doi.org/10.1021/bi00871a022>.
- 55 Slater EC. An evaluation of the Mitchell hypothesis of chemiosmotic coupling in oxidative and photosynthetic phosphorylation. *Eur J Biochem*. 1967;1:317–326. <https://doi.org/10.1111/j.1432-1033.1967.tb00076.x>.
- 56 Watt IN, Montgomery MG, Runswick MJ, Leslie AGW, Walker JE. Bioenergetic cost of making an adenosine triphosphate molecule in animal mitochondria. *P Natl Acad Sci USA*. 2010;107:16823–16827. <https://doi.org/10.1073/pnas.1011099107>.
- 57 Muller DJ, Dencher NA, Meier T, et al. ATP synthase: constrained stoichiometry of the transmembrane rotor. *FEBS Lett*. 2001;504:219–222. [https://doi.org/10.1016/S0014-5793\(01\)02708-9](https://doi.org/10.1016/S0014-5793(01)02708-9).
- 58 He JY, Ford HC, Carroll J, et al. Assembly of the membrane domain of ATP synthase in human mitochondria. *P Natl Acad Sci USA*. 2018;115:2988–2993. <https://doi.org/10.1073/pnas.1722086115>.
- 59 Bason JV, Montgomery MG, Leslie AGW, Walker JE. How release of phosphate from mammalian F-1-ATPase generates a rotary substep. *P Natl Acad Sci USA*. 2015;112:6009–6014. <https://doi.org/10.1073/pnas.1506465112>.
- 60 Wu F, Zhang EY, Zhang JY, Bache RJ, Beard DA. Phosphate metabolite concentrations and ATP hydrolysis potential in normal and ischaemic hearts. *J Physiol-London*. 2008;586:4193–4208. <https://doi.org/10.1113/jphysiol.2008.154732>.
- 61 Alpert NM, Guehl N, Ptaszek L, et al. Quantitative in vivo mapping of myocardial mitochondrial membrane potential. *PLoS One*. 2018;13. <https://doi.org/10.1371/journal.pone.0190968>. ARTN e0190968.
- 62 Wan B, Doumen C, Duszynski J, Salama G, Vary TC, Lanoue KF. Effects of cardiac work on electrical potential gradient across mitochondrial-membrane in perfused rat hearts. *Am J Physiol*. 1993;265:H453–H460.
- 63 Gerencser AA, Chinopoulos C, Birket MJ, et al. Quantitative measurement of mitochondrial membrane potential in cultured cells: calcium-induced de- and hyperpolarization of neuronal mitochondria. *J Physiol-London*. 2012;590:2845–2871. <https://doi.org/10.1113/jphysiol.2012.228387>.
- 64 Zhang H, Huang HM, Carson RC, Mahmood J, Thomas HM, Gibson GE. Assessment of membrane potential's of mitochondrial populations in living cells. *Anal Biochem*. 2001;298:170–180. <https://doi.org/10.1006/abio.2001.5348>.
- 65 Gurm GS, Danik SB, Shoup TM, et al. 4-[F-18]-Tetraphenylphosphonium as a PET tracer for myocardial mitochondrial membrane potential. *Jacc-Cardiovasc Imag*. 2012;5:285–292. <https://doi.org/10.1016/j.jcmg.2011.11.017>.
- 66 Pelletier-Galarneau M, Petibon Y, Ma C, et al. In vivo quantitative mapping of human mitochondrial cardiac membrane potential: a feasibility study. *Eur J Nucl Med Mol Imag*. 2020. <https://doi.org/10.1007/s00259-020-04878-9>.
- 67 Mitchell P. Coupling of phosphorylation to electron and hydrogen transfer by a chemi-osmotic type of mechanism. *Nature*. 1961;191:144–148.
- 68 Mitchell P. Possible molecular mechanisms of the protonmotive function of cytochrome systems. *J Theor Biol*. 1976;62:327–367.
- 69 Mitchell P. David Keilin's respiratory chain concept and its chemiosmotic consequences. *Nobel Prize Lect*. 1978;1:295–330.
- 70 Nelson D, Cox M. *Lehninger Principles of Biochemistry Textbook Pg 731-748*. sixth ed. WH Freeman and Company; 2013.
- 71 Garrett R, Grisham C. *Biochemistry Textbook Pg 659-661*. fifth ed. Brooks/Cole CENGAGE Learning, United States of America.; 2013.
- 72 Metelkine E, Demin O, Kovacs Z, Chinopoulos C. Modeling of ATP-ADP steady-state exchange rate mediated by the adenine nucleotide translocase in isolated mitochondria. *FEBS J*. 2009;276:6942–6955. <https://doi.org/10.1111/j.1742-4658.2009.07394.x>.
- 73 Arias-Hidalgo M, Hegermann J, Tsiavalariis G, et al. CO2 and HCO3- permeability of the rat liver mitochondrial membrane. *Cell Physiol Biochem*. 2016;39:2014–2024. <https://doi.org/10.1159/000447897>.
- 74 Cali T, Ottolini D, Brini M. Mitochondrial Ca2+ as a key regulator of mitochondrial activities. *Adv Mitochondrial Med*. 2012;942:53–73. https://doi.org/10.1007/978-94-007-2869-1_3.
- 75 Toth A, Meyrat A, Stoldt S, et al. Kinetic coupling of the respiratory chain with ATP synthase, but not proton gradients, drives ATP production in cristae membranes. *Proc Natl Acad Sci USA*. 2020;117:2412–2421. <https://doi.org/10.1073/pnas.1917968117>.
- 76 Strauss M, Hofhaus G, Schröder RR, Kühlbrandt W. Dimer ribbons of ATP synthase shape the inner mitochondrial membrane. *EMBO J*. 2008;27:1154–1160. <https://doi.org/10.1038/emboj.2008.35>.